

Search for LFV with the Mu3e experiment

Alexandr Kozlinskiy^{a,*} for the Mu3e Collaboration

^a*Institut für Kernphysik and PRISMA+ Cluster of Excellence,
Johannes Gutenberg-Universität Mainz,
Johann-Joachim-Becher-Weg 45, 55128 Mainz, Germany*

E-mail: akozlins@uni-mainz.de

The Mu3e experiment is designed to search for the lepton flavor violating decay $\mu^+ \rightarrow e^+ e^- e^+$. The ultimate aim of the experiment is to reach a branching ratio sensitivity of 10^{-16} . The experiment is located at the Paul Scherrer Institute (Switzerland) and an existing beam line providing 10^8 muons per second will allow to reach a sensitivity of a few 10^{-15} in the first phase of the experiment. In the middle of 2021 a successful Integration Run was performed with a reduced detector and a slice of the readout chain envisaged for the final detector. The design and prototyping of the detector is mostly finalized, the production of the sub-detectors is underway and the commissioning will start in the following years.

*** *The 22nd International Workshop on Neutrinos from Accelerators (NuFact2021)* ***
*** *6-11 Sep 2021* ***
*** *Cagliari, Italy* ***

*Speaker

1. Introduction

The Mu3e experiment [1] is designed to search for the lepton flavor violating decay $\mu^+ \rightarrow e^+e^-e^+$. The experiment is located at the Paul Scherrer Institute (PSI) and will use low-energy muons provided by the π E5 beam line at a rate of 10^8 muons per second. This rate will allow to reach a sensitivity of 2×10^{-15} in the first phase of the experiment. With the planned high intensity muon beam line the sensitivity will be further improved to the level of 10^{-16} .

The $\mu^+ \rightarrow e^+e^-e^+$ decay has an unobservable branching fraction of below 10^{-54} in Standard Model (SM). Consequently, any observation of such a decay will point to the presence of New Physics (NP). The current limit on $Br(\mu^+ \rightarrow e^+e^-e^+) < 10^{-12}$ at 90% C.L. was set by the SINDRUM [2] experiment about 30 years ago and the Mu3e experiment aims to improve this limit by 4 orders of magnitude.

2. Detector

Figure 1 shows a schematic view of the detector. In the middle, the central barrel of the detector is shown. The muons with a momentum of about 28 MeV/c are stopped and decay at rest on the muon stopping target surrounded by two inner layers of high-voltage monolithic active pixel sensors (HV-MAPS) [3] placed close to target to minimize the effect of multiple scattering on the vertex resolution. These sensors are 2×2 cm² with a thickness of 50 μ m, a pixel size of 80×80 μ m² and have an efficiency above 99% [4]. The decay products first pass through two inner layers and then through two outer pixel layers and a scintillating fibre detector placed just before the outer layers. The whole detector is placed in a solenoid magnet with a 1 T magnetic field. As the decay positrons and electrons have low energy, they can bend back into the pixel layers and produce additional hits that allow to improve the momentum resolution of the reconstructed particles. To increase the acceptance for such particles, two more detector stations are added upstream and downstream of the central station. These stations have a similar geometry to the central station but contain only double outer pixel layers and use a scintillating tile detector for time measurement. The signals from scintillating fibres and tiles are readout by silicon photomultipliers (SiPM) and digitized with a mixed-signal SiPM readout ASIC (MuTRiG [5]).

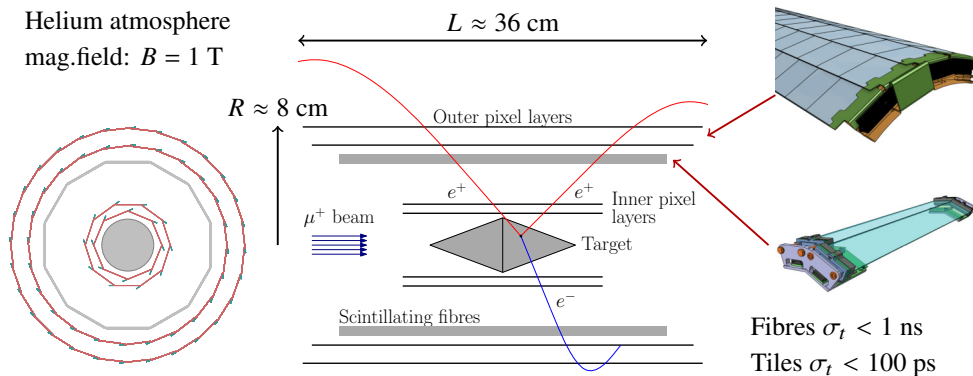


Figure 1: Schematic view of the Mu3e detector [1].

3. Detector readout

The Mu3e detector readout [6] has no hardware trigger and each sub-detector sends a continuous stream of data to the readout system. Due to high data rate it is not possible to store all the received data and the online reconstruction is used to reduce the data rate by a factor of 100.

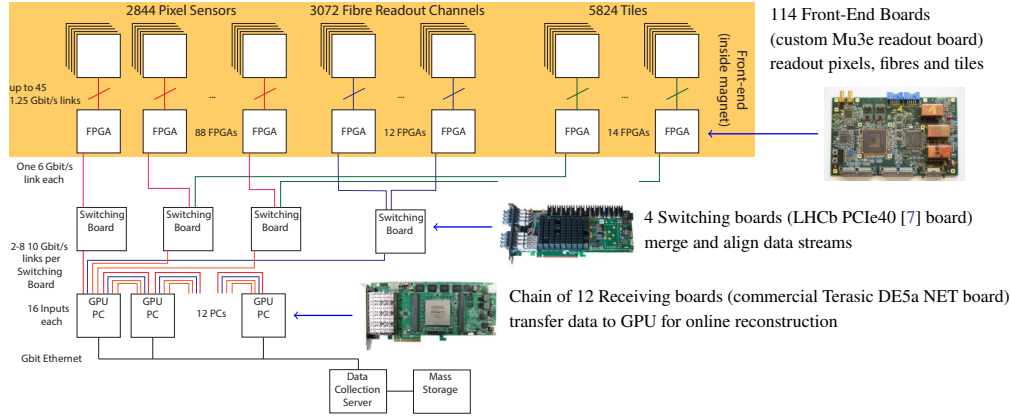


Figure 2: Schematic of the Mu3e readout system.

Figure 2 shows a schematic of the Mu3e readout system. The first layer of the readout consist of 114 Front-End Boards (FEBs) that receive data from the pixels as well as the fibre and tile detectors through low-voltage differential signaling (LVDS) links. The FEBs are located inside the magnet and send data through optical links to a second readout layer consisting of 4 Switching Boards outside of the detector area. The Switching Boards merge and align data streams and transmit optically to the Filter Farm. The Filter Farm consist of 12 PCs that house Receiving Boards chained together to receive data from the Switching Boards and GPUs that are used for online reconstruction.

4. Simulation, reconstruction and sensitivity

The detector simulation is based on Geant4 [8] implementing the detector as close as possible to the final geometry.

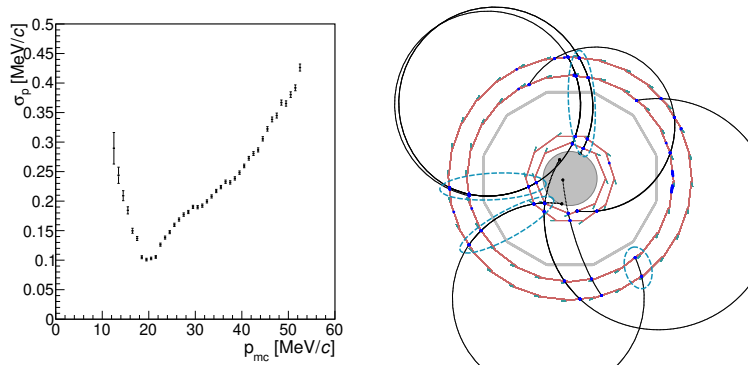


Figure 3: Momentum resolution of the reconstructed tracks (left) and display of reconstructed event (right).

The reconstruction algorithms are developed based on the above simulation and allow to reconstruct tracks within acceptance with high efficiency (about 90%) and excellent momentum resolution (see Figure 3).

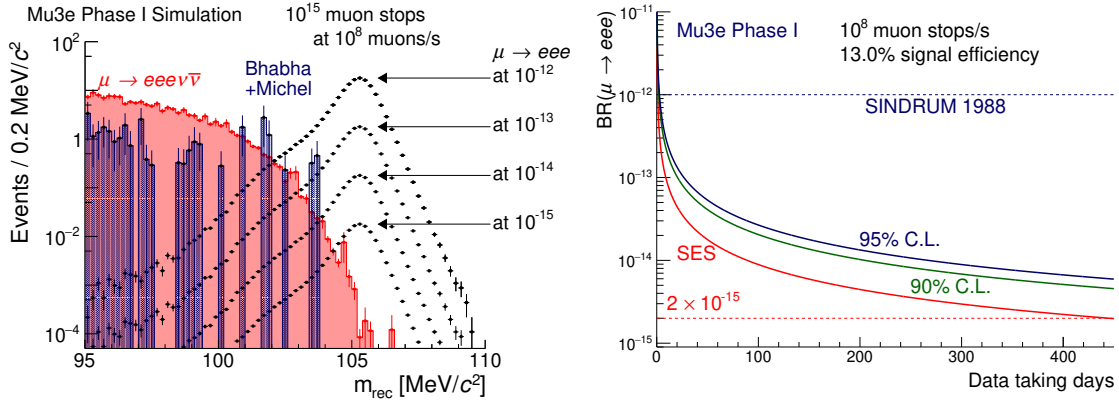


Figure 4: Invariant mass distribution (left) for signal and background and sensitivity (right).

Figure 4 (left) shows the invariant mass distribution for simulated signal events at different branching fractions (dots) and background that comes from a combination of particles from different sources (internal conversion, Bhabha pair production and Michel decay). The final sensitivity projection is shown in Figure 4 (right) showing that first phase of the Mu3e experiment will be able to reach a single event sensitivity of 2×10^{-15} within 400 days of data taking.

5. 2021 integration run

From May to July of 2021 a first Integration Run was performed at PSI with the goal of testing the readout and mechanical construction of a reduced detector consisting of two inner pixel layers and two ribbons of scintillating fibres.

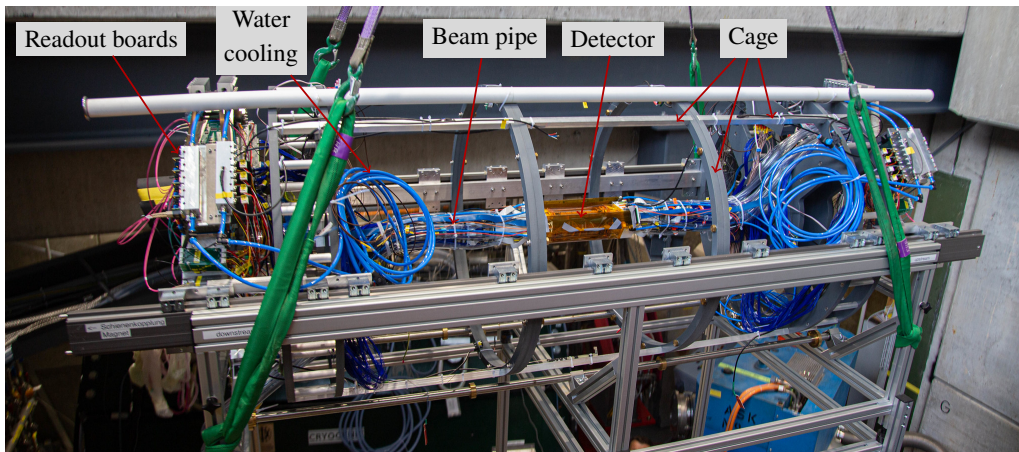


Figure 5: A photo of the detector during the 2021 Integration Run.

Figure 5 shows a photo of the integration run detector in the beam area during the craning just before insertion into the magnet. The detector was assembled in the detector cage with all

the readout electronics, services (cooling pipes), power converters, etc. The run was performed with a muon beam, gaseous helium cooling of the pixel detector and with and without magnetic field. The readout system was similar to the one envisaged for the final detector: the data from the pixels and fibres were readout with Front-End Boards, then sent optically to a Switching Board and subsequently to a Receiving Board housed in Filter Farm PC.

During integration run many components (mechanical and readout) were tested and provided feedback on necessary improvements.

6. Summary

The design and prototyping of the Mu3e detector is mostly finalized. A full description of the detector can be found in the recently published TDR [1].

The performance and sensitivity of the detector and its components was extensively tested in the labs, test beams and during the recent integration run, which was a success, showing the validity of many design decisions and providing feedback on necessary improvements of many components.

The existing simulation and reconstruction show that Mu3e experiment can reach a sensitivity of a few 10^{-15} within one year of data taking with the current detector design and geometry.

The production of the sub-detectors is under way and assembly and commissioning of the Mu3e detector will be performed in the following years.

References

- [1] K. Arndt *et al.* [Mu3e], Nucl. Instrum. Meth. A **1014** (2021), 165679 doi:10.1016/j.nima.2021.165679
- [2] U. Bellgardt *et al.* [SINDRUM], Nucl. Phys. B **299** (1988), 1-6 doi:10.1016/0550-3213(88)90462-2
- [3] I. Peric, Nucl. Instrum. Meth. A **582** (2007), 876-885 doi:10.1016/j.nima.2007.07.115
- [4] H. Augustin, N. Berger, S. Dittmeier, D. M. Immig, D. Kim, L. Mandok, A. M. Gonzalez, M. Menzel, L. O. S. Noehte and I. Perić, *et al.* JPS Conf. Proc. **34** (2021), 010012 doi:10.7566/JPSCP.34.010012 [arXiv:2012.05868 [physics.ins-det]].
- [5] W. Shen, T. Harion, H. Chen, K. Briggli, V. Stankova, Y. Munwes and H. C. Schultz-Coulon, IEEE Trans. Nucl. Sci. **65** (2018) no.5, 1196-1202 doi:10.1109/TNS.2018.2821769
- [6] H. Augustin *et al.* [Mu3e], IEEE Trans. Nucl. Sci. **68** (2021), 1833-1840 doi:10.1109/TNS.2021.3084060 [arXiv:2010.15648 [physics.ins-det]].
- [7] M. Bellato *et al.*, J. Phys. Conf. Ser. **513** (2014), 012023 doi:10.1088/1742-6596/513/1/012023
- [8] S. Agostinelli *et al.* [GEANT4], Nucl. Instrum. Meth. A **506** (2003), 250-303 doi:10.1016/S0168-9002(03)01368-8